IEEE Access
Multidisciplinary | Rapid Review | Open Access Journal

Received 4 June 2023, accepted 9 July 2023, date of publication 24 July 2023, date of current version 2 August 2023.

Digital Object Identifier 10.1109/ACCESS.2023.3298106

RESEARCH ARTICLE

An Enhanced P&O MPPT Algorithm With Concise Search Area for Grid-Tied PV Systems

AHMED ISMAIL M. ALI[1], (Member, IEEE), HOSSAM H. H. MOUSA[1], HASSANIEN RAMADAN A. MOHAMED[1], SALAH KAMEL[2], ABDURRAHMAN SHUAIBU HASSAN[3], ZUHAIR MUHAMMED ALAAS[4], (Member, IEEE), ESSAM E. M. MOHAMED[1], (Member, IEEE), AND ABDEL-RAHEEM YOUSSEF ABDALLAH[1]

[1]Electrical Engineering Department, South Valley University, Qena 83523, Egypt
[2]Electrical Engineering Department, Faculty of Engineering, Aswan University, Aswan 81542, Egypt
[3]Electrical Engineering Department, School of Engineering Technology, Soroti University, Arapai, Uganda
[4]Electrical Engineering Department, Jazan University, Jazan 45142, Saudi Arabia

Corresponding author: Abdurrahman Shuaibu Hassan (hassan.shvaibu@kiu.ac.ug)

ABSTRACT Due to improved efficiency of solar photovoltaic (PV) systems, this article proposes a modified perturb and observe (MPO) maximum power point tracking (MPPT) algorithm. The MPO algorithm in question adopts a tracking approach that divides the power-voltage curve into four operational regions based on the estimated open-circuit voltage. Additionally, this algorithm enhances the maximum power point (MPP) tracking method by reducing unnecessary step-size calculations, focusing only on a 10% section of the power-voltage curve that contains the MPP. Consequently, the two regions located far from the MPP, below 90% of the power-voltage range, utilize a large fixed step-size to ensure swift tracking speed. Furthermore, in the regions close to the MPP, the remaining areas employ a similar tracking strategy as the adaptive P&O algorithm, aiming to achieve minimal steady-state oscillations around the optimal MPP. The performance of the proposed MPO algorithm is demonstrated by validating it against sinusoidal, ramp irradiance, and one-day (10 hr.) irradiance profiles using MATLAB/SIMULINK. The simulation results confirm that the proposed algorithm outperforms recently published techniques in terms of convergence speed, achieving the shortest time of 15 ms, and slightly higher tracking efficiency of the PV system under uniform irradiation, reaching 99.8%.

INDEX TERMS PV system, large-scale PV array, grid-tied systems, MPPT, P&O, boost converter.

NOMENCLATURE

V_{MPP}	PV voltage at MPP.
V_{oc}	Open circuit voltage of PV array.
I_{ph}	Photo-generated current.
I_{sat}	Reverse saturation current.
I_{sc}	PV short circuit current.
G	Global insulation.
T_{eff}	Tracking efficiency.
BC	Boost converter.
MPPT	Maximum Power Point Tracking.
CPO	Conventional step-size P&O.
MPO	Modified P&O.
LS-PO	Large-step P&O.
SS-PO	Small-step P&O.

The associate editor coordinating the review of this manuscript and approving it for publication was Min Wang.

I. INTRODUCTION

The growing global power demand, resource depletion, and environmental concerns related to traditional energy sources have led to a significant push for the widespread adoption of renewable energy resources [1], [2], [3]. As a result, renewable energy sources such as wind, solar, tidal, and geothermal energy have emerged as sustainable and environmentally friendly alternatives to conventional resources. Among these, solar photovoltaic (PV) systems offer a promising solution for harnessing solar energy due to their simplicity, convenience,

scalability, pollution-free operation, and low maintenance requirements. However, a major drawback of PV systems is their relatively lower conversion efficiency of solar cells [4], [5]. Typically, solar cells have an efficiency ranging from 9% to 17%, which is influenced by weather conditions [6]. Moreover, the dependency of solar energy generation on weather conditions makes PV systems an unreliable power source. Therefore, efficient control strategies are crucial to ensure the effectiveness and reliability of PV system operation.

The I-V and P-V characteristics of solar cells are nonlinear and dependent on factors like applied radiation and temperature [7], [8]. As a result, there exists a specific point on the P-V curve known as the maximum power point (MPP), where the solar cell can extract the maximum power [9]. To operate at this MPP, maximum power point tracking (MPPT) algorithms have been developed and implemented in PV control systems. Various MPPT techniques have been introduced to track the MPP of solar panels under different irradiance profiles. These techniques can be broadly categorized into two main groups: conventional MPPT techniques and soft computing MPPT techniques. Conventional MPPT techniques, such as fractional short-circuit current, fractional open-circuit voltage, perturb and observe (P&O), and hill climbing strategies, are known for their simplicity and low implementation cost [1], [10].

The main limitations of fractional short-circuit current and fractional open-circuit voltage techniques are their low tracking accuracy and limited applicability in low power situations. Despite the widespread use and effectiveness of Hill climbing (HC), P&O, and Incremental Conductance (IC) methods under consistent sunlight, they are ineffective when faced with rapidly changing sunlight conditions and partial shading.

In addition, the primary limitations of conventional methods include slow tracking speed and significant steady-state oscillations. To address these shortcomings, soft computing techniques have been introduced, such as fuzzy logic control, sliding mode control, artificial neural networks, and metaheuristic-based algorithms like particle swarm optimization and genetic algorithms [11], [12], [13]. These approaches are effective in dealing with system nonlinearity and achieving the global optimum maximum power point, particularly in the presence of partial shading conditions. However, the use of soft computing MPPT techniques raises concerns regarding computational burden and complexity [14].

Various MPPT algorithms have recently been introduced for efficient tracking of PV-MPP [5], [15], [16]. In [17], a new IC-MPPT technique was presented for rapidly changing irradiance profiles, adjusting the DC-DC converter duty cycle. However, it has slower time response compared to other MPPT techniques. Reference [18] proposed an advanced P&O MPPT technique to improve system efficiency under fast-changing irradiation conditions. However, it exhibits relatively slow time response and high steady-state oscillations. Reference [19] suggested an improved IC-MPPT technique to enhance system dynamic response under fast-changing irradiance profiles. However, the presented topology requires a specialized controller, increasing system installation cost due to multiple calculations. [20] introduced a novel MPPT algorithm for accurate dynamic behavior and system efficiency. Nevertheless, it has a relatively slow MPPT speed. Reference [21] proposed a new MPPT technique using the photodiode as a current sensor, reducing the number of required sensors in PV systems. However, it is only applicable to simple configurations and low-power PV systems. Reference [2] presented a modified P&O MPPT algorithm to minimize steady-state oscillations by considering variable duty cycle perturbation step-size. Reference [22] proposed a novel MPPT technique based on the particle swarm optimization strategy, enhancing system tracking efficiency. However, it requires a controller with higher specifications, leading to increased installation cost. Reference [23] introduced an advanced MPPT technique based on scanning, while [24] proposed a novel hybrid MPPT technique based on direct P&O MPPT. Reference [25] suggested an improved auto-scaling variable step-size P&O MPPT technique for enhancing system dynamic response and stability. However, it complicates controller calculations, increases execution time, and requires a higher specification controller. Reference [26] presented an improved P&O MPPT technique with efficient open-circuit voltage estimation for grid-connected PV systems, utilizing variable step-size for duty cycle perturbation, reducing required sensors and enhancing steady-state oscillations. Reference [9] proposed an improved P&O MPPT technique for boosting PV system efficiency by concentrating the search area to 15% containing the MPP and starting perturbations within this limited search space. Furthermore, several computational-based MPPT algorithms have been suggested for efficient operation in standalone and grid-integrated applications [27], [28], [29], [30], [31]. However, they suffer from control complexity and increased controller execution time.

Based on a comprehensive review of existing literature, this paper introduces an advanced perturb and observe (P&O) MPPT technique that incorporates an adaptive duty cycle perturbation, resulting in a reduced search area. The proposed modified P&O (MPO) algorithm aims to minimize the computation of excessive step sizes by focusing the MPP tracking search area on only 10% of the power-voltage curve. To achieve this, the power-voltage curve is divided into four operating regions based on the estimated open-circuit voltage. The outer two regions, located far from the MPP and representing below 90% of the power-voltage range, utilize a large fixed step size, ensuring rapid tracking speed. The remaining regions, closer to the MPP, employ a methodology similar to the adaptive P&O algorithm to achieve low steady-state oscillations around the optimal MPP.

To validate the effectiveness of the proposed MPO algorithm, sinusoidal, ramp irradiance, and one-day

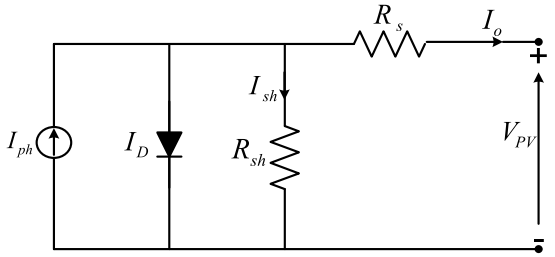

FIGURE 1. PV model [26].

(10 hr.) irradiance profiles are simulated using MATLAB/SIMULINK. The results demonstrate that the application of the proposed MPO algorithm enhances the system's tracking speed while minimizing steady-state oscillations. This confirms the superiority of the proposed algorithm compared to recently published techniques.

The article is structured as follows: Section II provides a mathematical model of the solar PV system. Section III focuses on the modeling of the boost converter. The grid side modeling is discussed in Section IV. In Section V, various P&O MPPT algorithms, including the conventional P&O algorithm, adaptive P&O algorithm, and the proposed MPO algorithm based on open circuit voltage estimation method, are examined. Section VI presents the simulation results of the proposed MPO algorithm using different solar radiation profiles. Section VII demonstrates the superior performance of the proposed MPO algorithm compared to recently published P&O algorithms. Finally, Section VIII summarizes the key findings of the article.

II. MODELING OF SOLAR CELL

Solar cells are crucial components in photovoltaic (PV) systems as they directly convert sunlight into electricity. They are connected in parallel and series combinations to increase the output voltage and current, creating solar arrays. In the literature, the commonly used solar cell models are the single diode and double diode models [1]. Figure 1 illustrates the equivalent circuit of a single diode model. Mathematically, the output voltage and current of a PV module can be described as follows:

$$I_0 = N_p I_{ph} - N_p I_{sat}\left[e^{\frac{q(V+R_s\cdot I_0)}{A\cdot k\cdot T\cdot N_s}} - 1\right] - N_p\left[\frac{q(V+R_s\cdot I_0)}{N_s\cdot R_{sh}}\right] \quad (1)$$

where I_0 is the output current of the PV array, V is the terminal voltage of the PV array, N_p and N_s are the parallel and series connected modules of the PV array, I_{ph} is the photo-generated current, I_{sat} is the reverse saturation current and R_s and R_{sh} are the series and shunt resistance of the PV module, respectively. k, q, A *and* T are the Boltzmann's constant, electron charge, p-n ideality factor and cell temperature, respectively.

The photo-generated current I_{ph}, which is function of the solar irradiance G and the cell temperature can be described

TABLE 1. Canadian CS5P-220M PV module characteristic.

Maximum power, P_{mpp}	220 W
Voltage at MPP, V_{mpp}	48.3159 V
Current at MPP, I_{mpp}	4.54758 A
Open circuit voltage, V_{oc}	59.2618 V
Short circuit current, I_{sc}	5.09261 A
Temperature, at STC	25^oC

mathematically as follows;

$$I_{ph} = \frac{G}{1000}(I_{sc} + K_i(T - T_i)) \quad (2)$$

where I_{sc} is the short circuit current at standard temperature and irradiance ($G = 1000$ W/m^2 and $T_i = 298$ K), k_i is the short circuit current temperature coefficient and T_i is the cell reference temperature. The reverse saturation current varies with cell temperature and it is described as follows;

$$I_{sat.} = \frac{I_{sc} + K_i(T - T_i)}{\exp\left(\frac{V_{oc}+K_v(T-T_i)}{V_t}\right) - 1} \quad (3)$$

Where V_{oc} is the open-circuit voltage, K_v is the open-circuit voltage coefficient and V_t is the thermal voltage ($V_t = K.T/q$). The short-circuit current is expressed in terms, of irradiation G and temperature T:

$$\mathrm{I_{sc}}\,(G,T) = \frac{\mathrm{G}}{\mathrm{G_{(stc)}}}[\mathrm{I_{sc(stc)}} + \mu_{\mathrm{I_{sc}}}\left(T - \mathrm{T_{(stc)}}\right)] \quad (4)$$

The open-circuit voltage is expressed in terms, of irradiation G and temperature T () [2]:

$$\mathrm{V_{oc}}\,(G,T) = \mathrm{V_{oc(stc)}} + \mathrm{C_1}\ln\left(\frac{\mathrm{G}}{\mathrm{G_{(stc)}}}\right) + \mathrm{C_2}\ln\left(\frac{\mathrm{G}}{\mathrm{G_{(stc)}}}\right)^2 + \mathrm{C_3}\ln\left(\frac{\mathrm{G}}{\mathrm{G_{(stc)}}}\right)^3 + \mu_{\mathrm{V_{oc}}}\left(T - \mathrm{T_{(stc)}}\right) \quad (5)$$

where the constants values as follow; $C_1 = 5.468511 \times 10^{-2}$, $C_2 = 5.973869 \times 10^{-3}$, and $C_3 = 7.616178 \times 10^{-4}$ for silicon. $\mathrm{I_{sc}}$ and $\mathrm{I_{sc(stc)}}$ are short-circuit current of a PV module and its value at standard test conditions , $\mathrm{V_{oc}}$ and $\mathrm{V_{oc(stc)}}$ are the open-circuit voltage of a PV module and its voltage at standard test conditions.

G and $\mathrm{G_{(stc)}}$ are solar irradiance (W/m^2) and irradiance at standard test conditions (STC) (1000 W/m^2). T and $\mathrm{T_{(stc)}}$ are the temperature of the PV module (K) and its temperature at STC (25^{o}C or 298.15 K). $\mu_{\mathrm{V_{oc}}}, \mu_{\mathrm{I_{sc}}}$ are the thermal coefficient of the open-circuit voltage (V/^{o}C) and short-circuit current (A/^{o}C). A PV array composed of 60 modules based on the Canadian CS5P-220M PV module is used in this study. The module characteristics at fixed irradiance level of 1000 w/m^2 are presented in Table. 1.

III. MODELING OF BOOST CONVERTER

The PV module and grid-side inverter are connected through a step-up chopper, also known as a boost converter. This

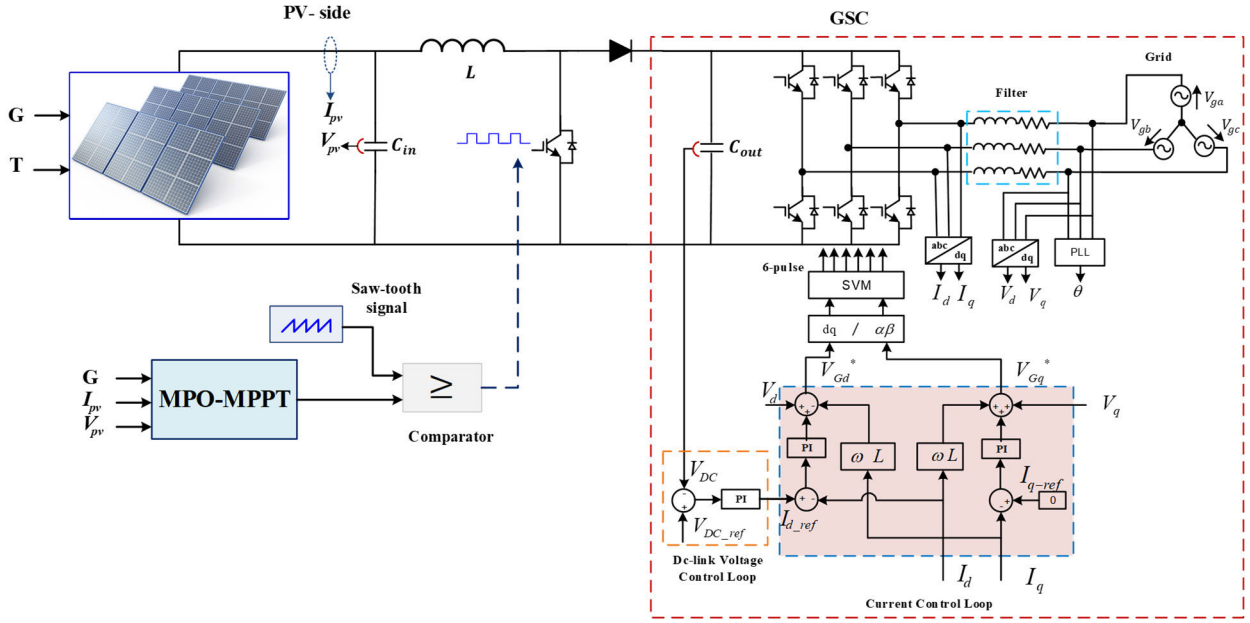

FIGURE 2. The proposed grid-connected system [26].

converter consists of a PWM-controlled IGBT switch, an input inductor, an output capacitor, and a diode (refer to Fig. 2). The primary purpose of the boost converter is to track the MPP as the irradiance level changes. Additionally, it boosts the output voltage from the PV module to a suitable level for grid connection. The IGBT switch can be toggled between ON and OFF states, and by adjusting its duty cycle, the output voltage can be controlled. The switch position is denoted by a switching state variable (u), which is set to zero when the switch is open and one when it is closed. The dynamic behavior of the boost converter can be described using Kirchhoff's laws [34].

$$\frac{di_L}{dt} = \frac{V_{pv} - V_o}{L} + \frac{V_o}{L} * u \tag{6}$$

$$\frac{dV_o}{dt} = \frac{i_L}{C_o} - \frac{i_L}{C_o} * u \tag{7}$$

where;

$$u = \begin{cases} 0, & IGBT\ is\ swiched - OFF \\ 1, & IGBT\ is\ switched - ON \end{cases}$$

where, V_o is the boost converter output voltage and i_L is the input inductor current. The output voltage V_o is function of the PV array voltage V_{pv} and the duty cycle D as expressed in (8) [1].

$$\frac{V_o}{V_{pv}} = \frac{1}{1 - D} \tag{8}$$

IV. GRID SIDE CONTROL

The PV generation system is linked to the grid using a grid-side inverter (GSI). The GSI plays a crucial role in controlling the active and reactive power injected into the grid, while also regulating the DC bus voltage to its reference value, even in changing weather conditions. The regulation of the DC voltage is achieved through a DC voltage control loop, which incorporates a PI outer controller loop. On the other hand, the control of the active and reactive power injected into the grid is carried out using an inner vector control loop. This control loop utilizes two PI controllers to regulate the d-axis and q-axis currents.

To achieve the unity power factor operation of the GSI, the quadrature current reference I_{q-ref} is set to zero. The block diagram of the grid-side control is depicted in Fig. 2. The phase voltages of the GSI as a function of grid voltages and currents are formulated in Eq. (9).

$$\begin{bmatrix} V_a \\ V_b \\ V_c \end{bmatrix} = [R_f] \begin{bmatrix} i_a \\ i_b \\ i_c \end{bmatrix} + \begin{bmatrix} \dot{\lambda}_a \\ \dot{\lambda}_b \\ \dot{\lambda}_c \end{bmatrix} + \begin{bmatrix} V_{ga} \\ V_{gb} \\ V_{gc} \end{bmatrix} \tag{9}$$

where V_a, V_b and V_c are the GSI output voltages, V_{ga}, V_{gb} and V_{gc} are the grid phase voltages. i_a, i_b and i_c are the grid line currents. $\dot{\lambda}_a = L_f \frac{di_{fa}}{dt}$, $\dot{\lambda}_b = L_f \frac{di_{fb}}{dt}$ and $\dot{\lambda}_c = L_f \frac{di_{fc}}{dt}$, R_f and L_f are the filter resistance and inductance, respectively. By transforming Eq. (9) from the stationary ABC phase coordinate system to the dq rotating coordinate system. The grid voltages are formulated as:

$$\begin{bmatrix} V_{gd} \\ V_{gq} \end{bmatrix} = \begin{bmatrix} V_d \\ V_q \end{bmatrix} - [r_f] \begin{bmatrix} i_d \\ i_q \end{bmatrix} - \begin{bmatrix} \dot{\lambda}_d - \omega_g \psi_q \\ \dot{\lambda}_q + \omega_g \psi_d \end{bmatrix} \tag{10}$$

Where (V_{gd}, V_{gq}) and (V_d, V_q) are the d-axis and q-axis of the grid voltages and GSI voltages, respectively. $\omega_g = 2\pi f_g$, $\psi_q = l_f i_q$, $\psi_d = l_f i_d$, $\dot{\lambda}_d = l_f \frac{d}{dt} i_d$, $\dot{\lambda}_q = l_f \frac{d}{dt} i_q$. The instantaneous active and reactive power injected to the grid

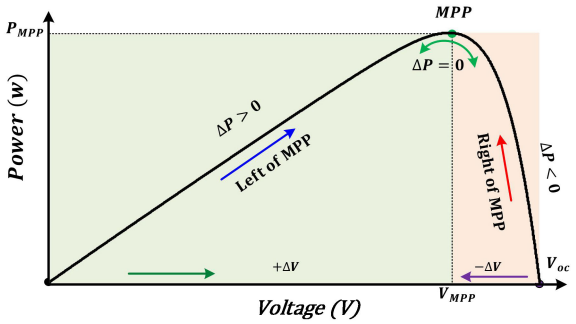

FIGURE 3. Conventional P&O MPPT technique [26].

TABLE 2. Scheme of the conventional P&O algorithm.

Sign of ΔP	Sign of ΔV	Resulting Perturbation
Positive	Positive	+ve
Positive	Negative	-ve
Negative	Positive	-ve
Negative	Negative	+ve

are given by:

$$P_g = \frac{3}{2}(V_{gd} i_{d-} V_{gq} i_q) \tag{11}$$

$$Q_g = \frac{3}{2}(V_{gd} i_{q-} V_{gq} i_d) \tag{12}$$

V. MPPT CONTROL

A. CONVENTIONAL P&O ALGORITHM [1]

The Conventional Perturb & Observe (CPO) algorithm is widely adopted due to its simplicity, as depicted in Fig.3. The strategy of the CPO algorithm can be summarized as follows:

- Continuously observe power variations (ΔP).
- Perturb the reference voltage until the maximum power point (MPP) is tracked.

During the tracking process, the direction of voltage perturbation is determined by the sign of ΔP. If ΔP is positive, the voltage perturbation continues in the same direction. Conversely, if ΔP is negative, it indicates that the MPP is far away, and the voltage perturbation should be reduced to track the MPP. Table 2 provides a summary of the CPO algorithm's operations.

The oscillation levels around the MPP and the settling time response are determined by the amplitude of the voltage or duty cycle step size used in the CPO algorithm. Therefore, the CPO algorithm utilizes a fixed step size, which can be either small or large. When a small step size is employed, it results in lower steady-state oscillation levels but slower convergence time and increased power loss. On the other hand, using a large step size reduces the convergence time but leads to higher oscillation levels. Consequently, several researchers have explored modifications to the CPO algorithm to address the limitations of response time and steady-state oscillation levels.

B. ADAPTIVE P&O ALGORITHM [2]

To overcome the limitations of conventional P&O algorithms, various adaptive P&O algorithms have been developed, utilizing either duty cycle or voltage perturbation approaches [4], [5], [6], [7]. These adaptive algorithms aim to address issues related to dynamic tracking response and steady-state oscillations. They intelligently adjust the perturbation step size during the tracking process based on the proximity to the MPP. In order to maximize tracking speed, a large perturbation step size is used when the operating point is far from the MPP. As the operating point gets closer to the MPP, the perturbation step size is dynamically reduced to a smaller value. Adaptive P&O algorithms employ varying perturbation step sizes according to the operating point, allowing for fast tracking with minimal steady-state oscillations.

In a specific study [35], the adaptation of the perturbation step size is achieved through a relationship between the variations in power (ΔP) and voltage (ΔV).

$$\Delta V_{n+1} = M \frac{\Delta P_n}{\Delta V_n} \tag{13}$$

where, M is an accuracy constant.

Another method can be used in [7] which mainly based on the logarithmic function,

$$\Delta V_{n+1} = M \ln\left(\frac{\Delta P_n}{\Delta V_n}\right) \tag{14}$$

Adaptive P&O algorithms provide fast dynamic response and good steady-state stability. However, they require additional calculations when operating far from the MPP. To reduce these calculations, a fixed step-size can be used in the far region from the MPP, resulting in a smaller search area for the MPP curve where adaptive step-size is applied.

C. PROPOSED P&O ALGORITHM

To overcome the limitations of the CPO method and minimize the computational burden associated with step-size calculations in adaptive perturb and observe (P&O) algorithms, the authors have introduced a modified P&O (MPO) algorithm in their research. This MPO algorithm offers a rapid dynamic response with minimal steady-state oscillations, while maintaining simplicity. The approach employed in the proposed MPO algorithm involves dividing the power-voltage curve into four operating regions based on an estimated open circuit voltage. The two regions located far from the maximum power point (MPP) employ a larger fixed step-size, enabling faster tracking speed and reducing unnecessary step-size calculations. On the other hand, the remaining regions closer to the MPP operate similarly to the adaptive P&O algorithm, resulting in reduced steady-state oscillations around the peak point. By combining elements from both the CPO and adaptive P&O algorithms, the proposed MPO algorithm effectively addresses their drawbacks and improves dynamic response performance. However, a significant challenge in implementing the MPO

TABLE 3. Literature review defined the factor K_{OC}.

Ref.	K_{oc}
[2]	0.65
[9]	0.76
[33]	0.70: 0.80
[34]	0.71 :0.78
[35]	0.75
[11]	0.76 (± 2%)
[12]	0.71
[13]	0.75: 0.78
[14]	0.76 (± 1%)

algorithm lies in accurately determining the values of the open circuit voltage and maximum output voltage.

1) ESTIMATING THE OPEN CIRCUIT AND MAXIMUM OUTPUT VOLTAGES

To implement the proposed MPO algorithm effectively, it is crucial to initially determine the values of VMPP (output voltage at maximum power) and VOC (open circuit voltage) for each solar radiation. This helps in dividing the MPP tracking curve into different operating search areas, allowing individual control over their applied step-size and tracking strategy. Numerous literature reviews indicate that the output voltage at maximum power VMPP is directly proportional to the open circuit voltage VOC, expressed as follows:

$$V_{MPP} = K_{oc} V_{oc} \tag{15}$$

where, K_{oc} is constant that determined based on the characteristics of the PV array and can be found in Table 3. The proposed method described in [26] can be employed to estimate the open circuit voltage, enabling the direct determination of the output voltage at maximum power using (15) with being approximately 0.76. This reduction in the number of required voltage and current sensors decreases the implementation cost of the PV system. Both VMPP and VOC are determined for the tracking strategy in the proposed MPO algorithm.

2) IMPLEMENTATION OF THE PROPOSED MPO ALGORITHM

Upon determining the open circuit voltage and the output voltage at maximum power, the power-voltage curve is divided into four regions. The objective of the proposed MPO algorithm is to restrict the search space for the maximum power point (MPP) within only 10% of the power-voltage curve. This approach enhances both the tracking speed and the reduction of steady-state oscillations around the MPP.

Specifically, Area (1) and Area (4) correspond to 90% of the power-voltage curve area. In these regions, a large fixed step-size is employed since the operating point is situated far from the MPP. The purpose is to minimize the response time.

TABLE 4. Search area distribution of power-voltage curve.

		Starting (% of Voc)	Ending (% of Voc)	Total area (% of Voc)
Area (1)	+ve	0	90	90
Area (2)		90	100	10
Area (3)	-ve	90	100	10
Area (4)		0	90	90

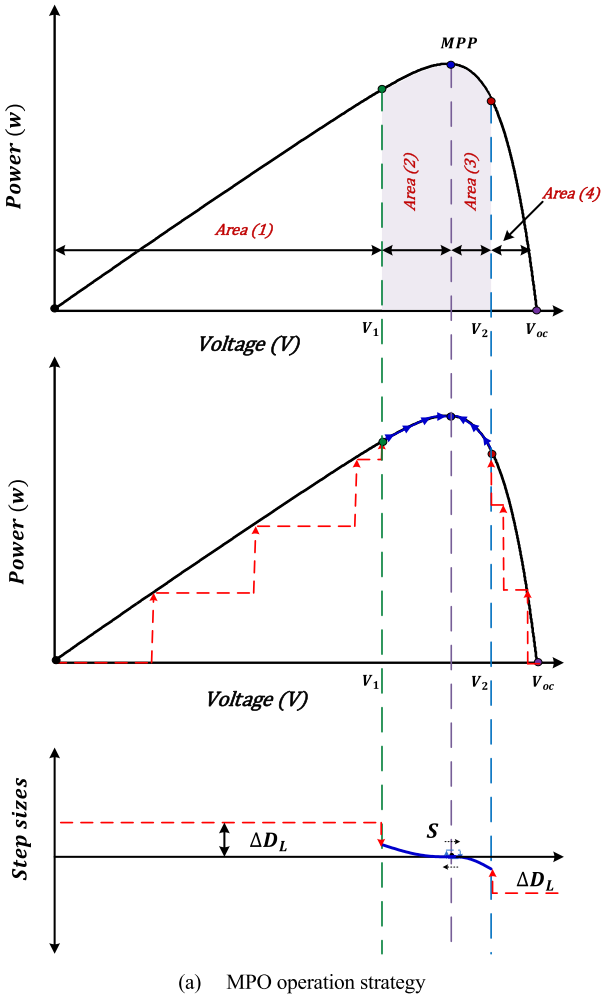

(a) MPO operation strategy

FIGURE 4. MPO algorithm strategy.

The duty cycle value is perturbed with ΔD_L if the operating voltage (V_{pv}) is ($0 < V_{pv} < V_1$) and ($V_2 < V_{pv} < V_{oc}$). The magnitudes of V_1 and V_2 are defined and tuned, as discussed in the literature review, to obtain the best performance of the proposed MPO algorithm as given in Table 4. By moving towards the MPP, the search area is limited to 10%. Area (2) and Area (3) are operated as same as the strategy of the adaptive P&O algorithm that reduces the steady-state oscillations. Hence, the duty cycle step-size is perturbed with value S. The magnitude of S is calculated as Eq. (16). Area (2) is defined when $V_1 < V_{pv} < V_{MPP}$, while Area (3) is defined when $V_{MPP} < V_{pv} < V_2$. The approach of the proposed MPO algorithm is shown in Fig.4 (a) while

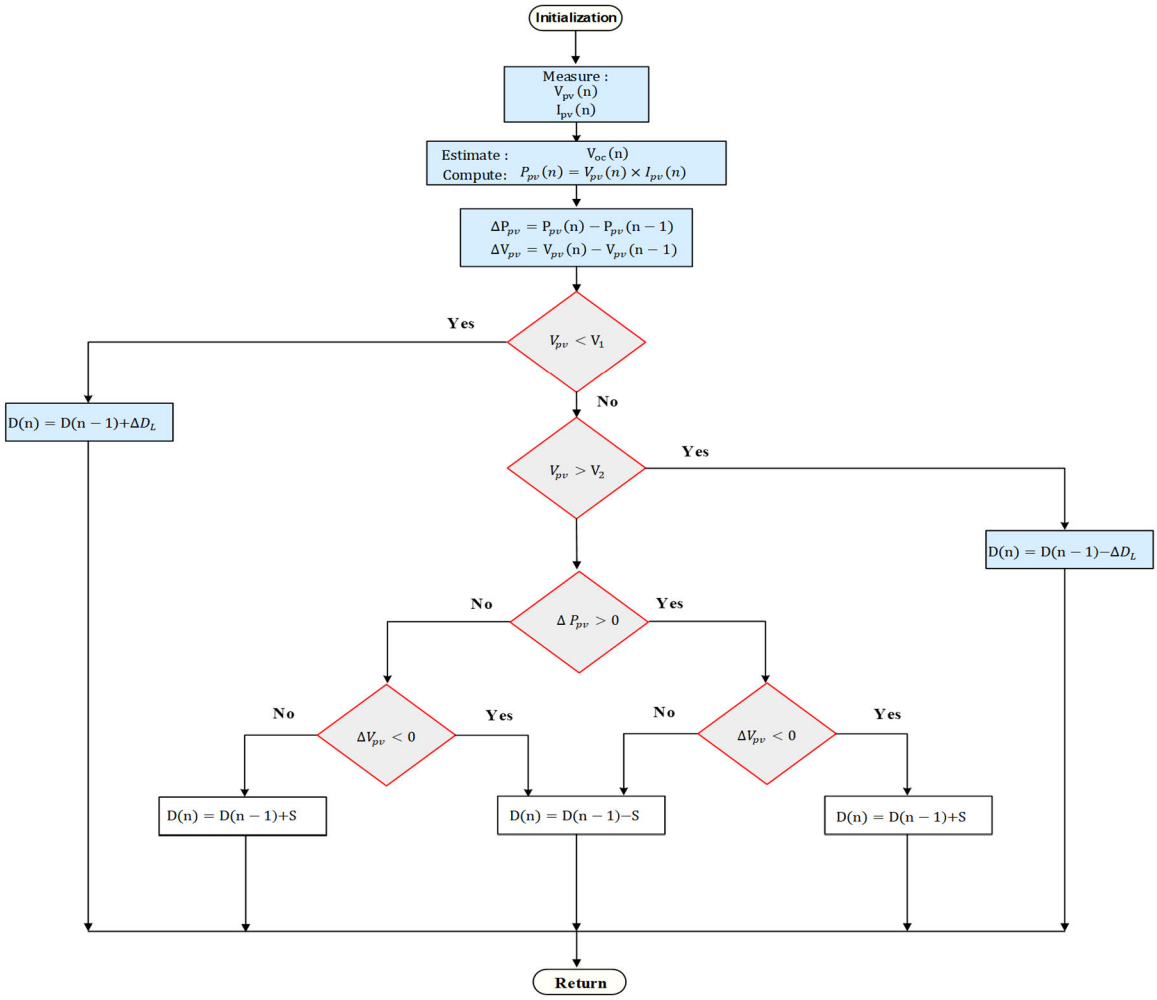

(b) Flow chart of MPO strategy.

FIGURE 4. *(Continued.)* **MPO algorithm strategy.**

the complete operation flow chart is given in Fig.4 (b).

$$S = M \frac{\Delta P_n}{\Delta V_n} \tag{16}$$

The operational approach of the proposed MPO algorithm can be summarized as follows:

- Estimating the V_{oc}..
- Dividing the power-voltage curve into four regions.
- Designating the two regions that are farther away from the MPP to be operated with a large fixed step-size.
- For the remaining regions closer to the MPP, employing an adaptive P&O algorithm.
- Perturbing the duty cycle using an appropriate step-size.
- Updating the control variables accordingly.

VI. RESULTS AND DISCUSSION

The grid-tied PV system is modeled and the effectiveness of the Proposed MPO algorithm is validated using the MATLAB/SIMULINK environment. The parameters of the overall system and the characteristics of the simulated PV array can be found in Appendix [1]. The performance of the developed MPO algorithm is evaluated under various solar irradiance profiles, including step change, sinusoidal, and real solar irradiance profiles, all at an ambient temperature of 25 °C. The results obtained from the proposed MPPT algorithm are compared with those obtained from the conventional P&O algorithm, both with large and small step sizes.

Furthermore, grid-side results are showcased to illustrate the effectiveness of the proposed MPO algorithm.

A. THE ROPP TEST

The proposed algorithm is tested under varying solar insolation conditions, both gradual changes and sudden step and ramp changes. Figure 5(a) shows the solar insolation profile used for testing. Figure 5(b) displays the output power of the PV system with both the conventional and proposed MPO algorithms.

Using the large step conventional P&O (LS-PO) algorithm results in high tracking speed (15 ms), but it also leads to large

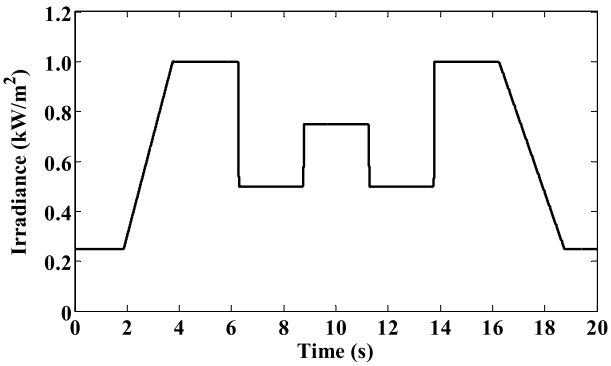

a) Ropp irradiance profile

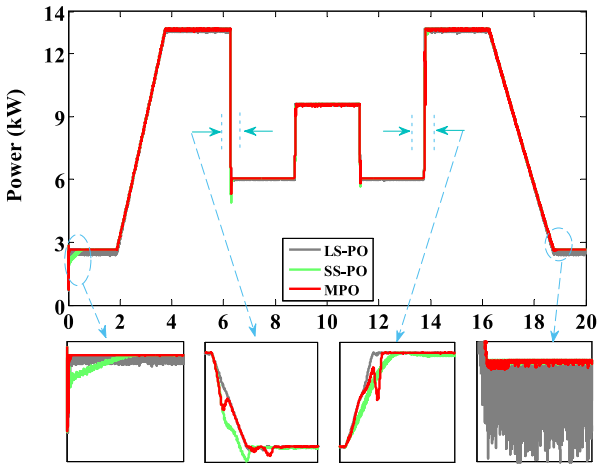

b) PV output-power

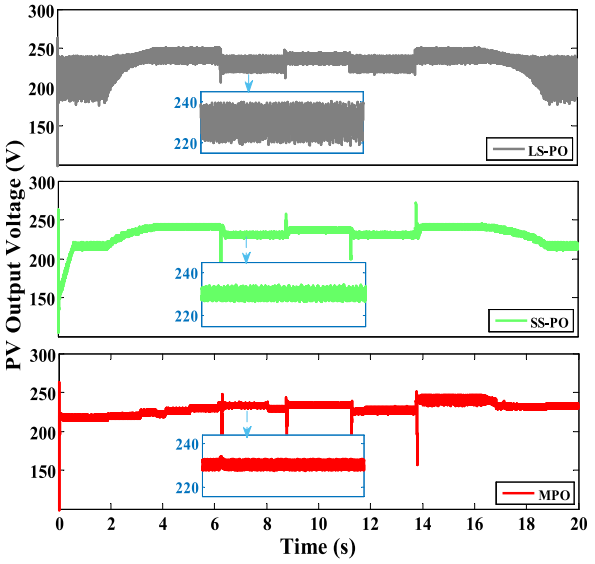

c) PV output voltage

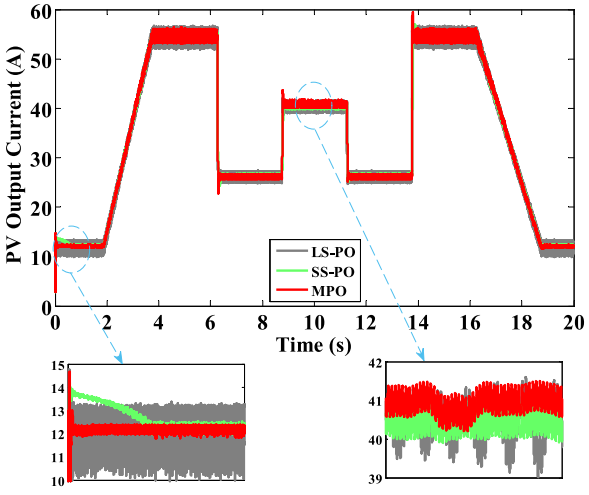

d) PV output current

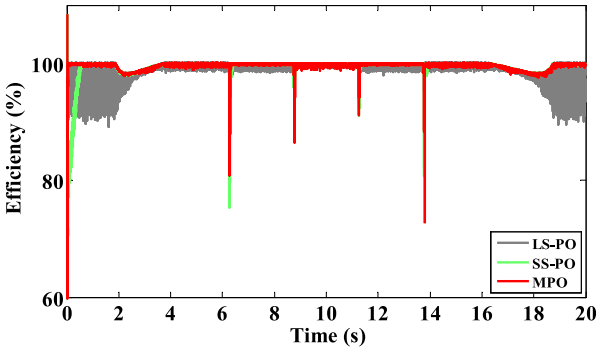

e) Tracking efficiency

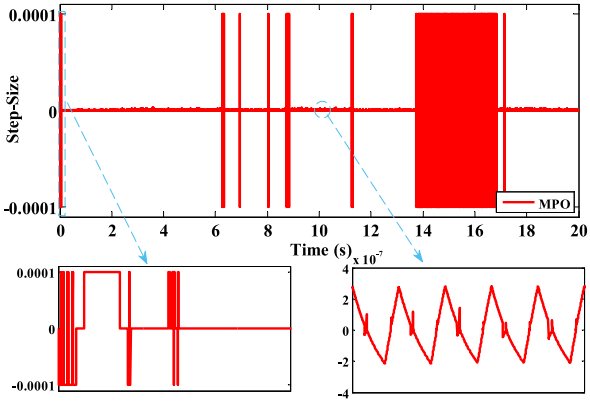

f) Perturbation step-size.

FIGURE 5. MPO algorithm strategy.

oscillations around the maximum power point (MPP), which reduces overall system efficiency.

On the other hand, the small step conventional P&O (SS-PO) algorithm eliminates steady state oscillations compared

to LS-PO, but the tracking speed drops significantly (120 ms) due to the smaller step size.

The proposed MPO algorithm combines the advantages of both LS-PO and SS-PO. It achieves a tracking speed similar to LS-PO (15 ms) while significantly reducing power oscillations even more than SS-PO, thanks to the adaptive step.

The performance analysis of the proposed technique can be further conducted by examining the solar array output voltage, as shown in Figure 5(c). The peak-to-peak voltage ripple for the conventional techniques with large and small fixed steps is observed to be 20 V and 3 V, respectively, as indicated in the zoomed region. In contrast, when applying the proposed algorithm, a smaller voltage ripple of 2 V is experienced, as depicted.

The superiority of the proposed MPO algorithm becomes evident in Figure 5(d), which illustrates the PV output current. Comparing with the conventional techniques, the proposed algorithm exhibits improved tracking efficiency.

Figure 5(e) presents the efficiency of the conventional and proposed MPO techniques over the operation period, calculated according to the reference [1]. Due to large steady-state oscillations, the conventional large fixed step P&O technique demonstrates lower efficiency compared to both the small step P&O and the proposed algorithm. The average efficiency values for the conventional large and small fixed step algorithms are 98.8% and 99.3%, respectively. However, the proposed technique achieves higher average efficiency at 99.8% due to its fast tracking response and smaller steady-state oscillations.

To validate the strategy of the proposed MPO algorithm, the perturbation duty cycle step-sizes are depicted in Figure 5(f), as investigated in section V-C. It is noteworthy that the large fixed step-size is utilized below 90% of the power-voltage curve, while closer to the MPP, adaptive step-sizes are employed, with the smallest values being ±2e-7.

A summarized comparison of the three tracking algorithms in terms of voltage ripple, settling time, and tracking efficiency is provided in Table 5.

The proposed MPO algorithm was used to evaluate the performance of the analyzed system on the grid side. This evaluation involved examining the power injected into the grid, as well as the voltages and currents, including the dc-link voltage. The results of the grid side analysis with the proposed algorithm can be seen in Fig.6. The performance of the dc-link voltage is shown in Fig.6 (a), where the capacitor dc voltage remains at the reference value of 750 V regardless of changes in irradiance levels. Fig.6 (b) displays the total active and reactive power injected into the grid. It is evident that the active power varies according to solar irradiance changes, while the reactive power remains close to zero due to the unity power factor operation of the grid side inverter. This can be observed in Fig.6(c), which illustrates that the voltage and current are always in phase. Additionally, Fig.6(d) demonstrates that the q-axis current remains at zero, while the d-axis component follows the reference value.

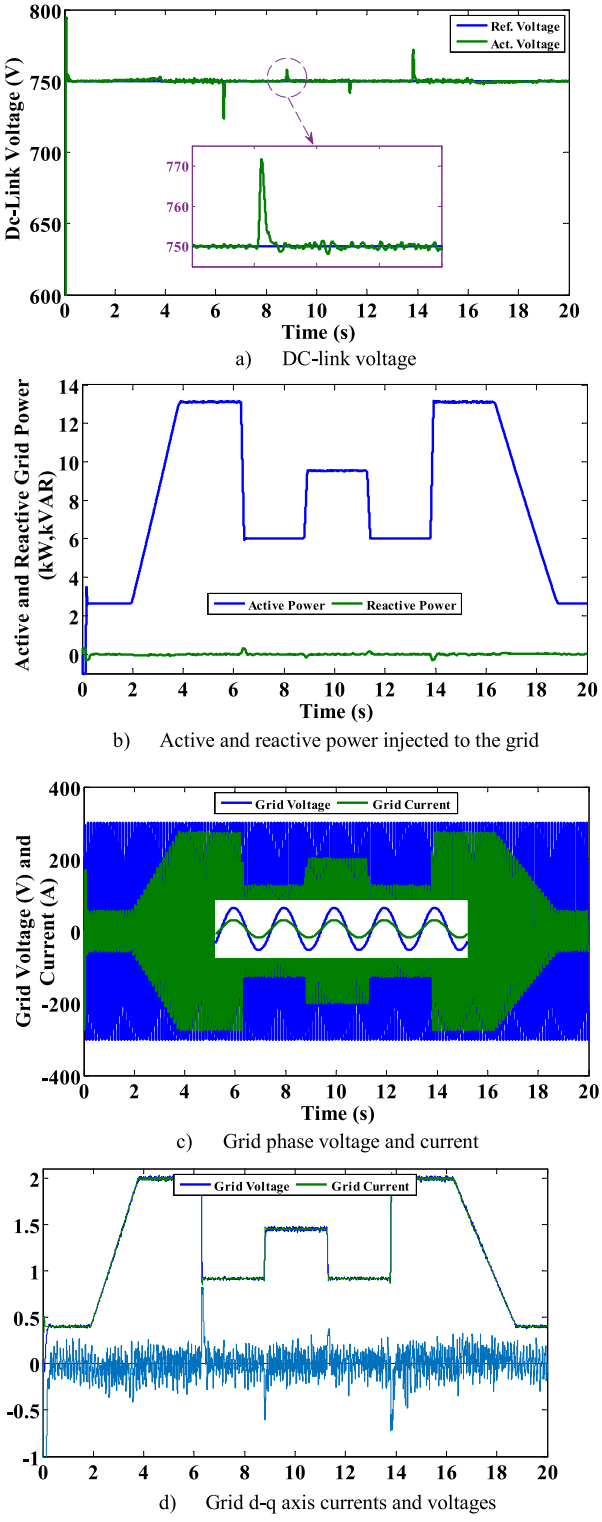

FIGURE 6. Grid-side system results.

B. SINE IRRADIANCE PROFILE

To evaluate the tracking performance of the proposed algorithm under real environmental conditions, a sinusoidal irradiance profile, as shown in Figure 7(a), is applied. This

TABLE 5. Comparison among CPO and MPO algorithms.

P&O algorithm	Voltage ripple (V) (Peak to Peak)	Perturbation step-size		Settling time (ms)	Tracking efficiency (%)
Conventional LS-PO	20	$\Delta V_1 = 1e-4$	Voltage perturbation	15	98.8
Conventional SS-PO	3	$\Delta V_2 = 1e-6$		120	99.3
Proposed MPO	~2	Section V.C	Duty cycle perturbation	15	99.8

TABLE 6. Comparison between the proposed algorithm and the recent published techniques.

Ref.	Tracker Algorithm	Control Variable	Online/ Offline	Complexity	Converter type	Convergence Speed (ms)	Tracking Efficiency (%)
[36]	Open-circuit voltage (OCV)	Voltage	Offline	Low	Buck converter	82	86
[37]	P&O	Voltage	Online	Low	Boost converter	76 (fixed step), 15 (variable step)	88.96
[38]	Short-circuit current (SCC)	Voltage	Offline	Low	Cuk converter	80	83
[39]	P&O IC	Duty cycle	Online	Low	Buck converter	50 60	97 97.8
[9]	P&O	Duty cycle	Online	Moderate	Boost converter	Not reported	Not reported
[22]	PSO-ANFIS P&O-ANFIS ANN	Voltage	Offline	High	Boost converter	10,000–17,000 12,000–19,000 13,000–19,000	97–98 85–97 85–97
[20]	Not reported	Voltage	Online	Moderate	Buck converter	12	99.6
[40]	IC	Duty cycle	Online	Low	Boost converter	81	95
[26]	P&O	Voltage	Online	Low	Boost converter	17	99.7
[27]	ABC	Voltage	Offline	High	Boost converter	160	98.92
[28]	ANN IBA-FLC	Voltage Voltage	Offline Offline	High High	Boost converter Boost converter	140 110	98.25 99.23
[29]	HWO-PS	Voltage	Offline	High	VSI	130	98.30
[30]	MRAC	Voltage	Offline	Moderate	Boost converter	4	99.6
[31]	WOA	Voltage	Offline	High	Boost converter	28	98.92
	GWO	Voltage	Offline	High	Boost converter	17.5	99.50
	PSO	Voltage	Offline	High	Boost converter	27	98.10
This article	**Modified P&O**	**Duty cycle**	**Online**	**Low**	**Boost converter**	**15**	**99.8**

profile introduces nonlinear changes in solar irradiance, in contrast to the linear changes analyzed in the previous profile. Figure 7(b) illustrates the output power obtained from the conventional and proposed MPPT algorithms. It is evident that the proposed algorithm exhibits superior tracking performance in terms of both tracking speed and steady-state oscillations compared to the conventional techniques. Upon closer examination of the zoomed regions, it can be observed that the algorithm with a large fixed step size suffers from incorrect tracking direction and higher steady-state oscillation. On the other hand, the algorithm with a small fixed step size experiences lower tracking speed as its main drawback.

C. ONE-DAY IRRADIANCE PROFILE

To further evaluate the proposed MPO technique, a daily irradiance profile spanning ten hours is utilized, as depicted in Fig.8 (a). This profile represents actual irradiance data for a day characterized by intermittent clouds and showers. The solar irradiance gradually increases in the morning, remains relatively stable during the afternoon, and then linearly decreases in the late afternoon. Fig.8 (b) illustrates the output power, enabling a comparison of the tracking performance between the conventional and proposed algorithms.

Both the conventional and proposed algorithms are capable of tracking the maximum power point (MPP). However, the conventional algorithm with a large fixed step P&O

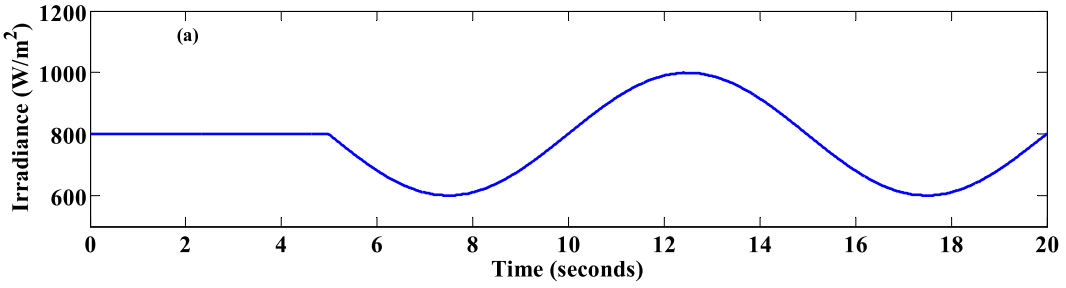

a) Sinusoidal irradiance profile

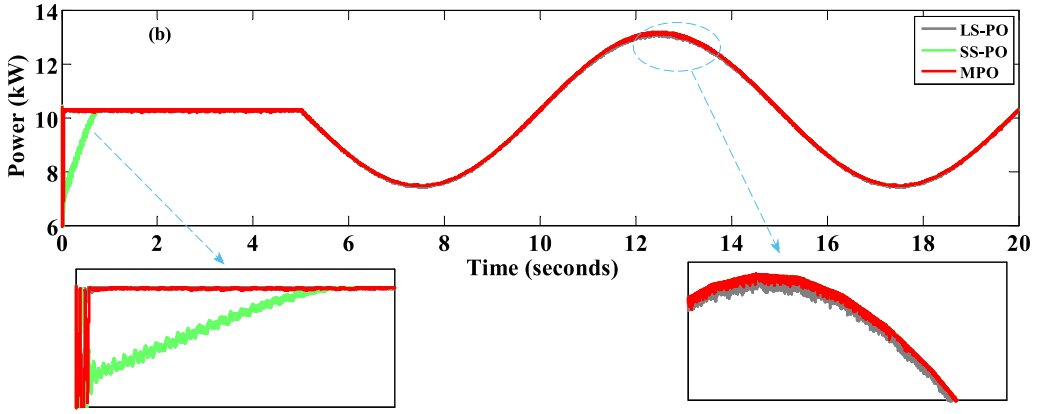

b) PV output voltage

FIGURE 7. Results of sine irradiance profile.

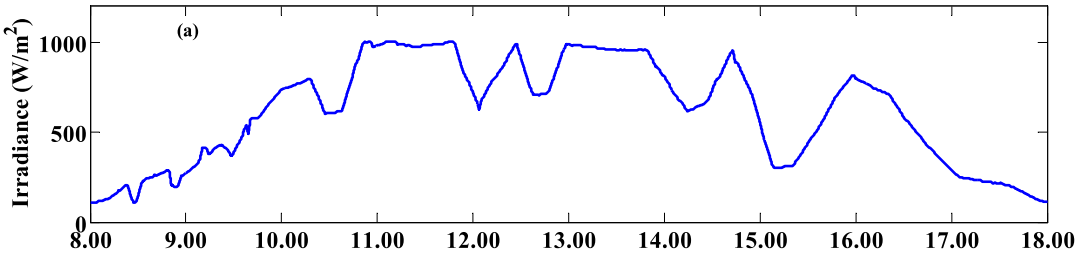

a) One-day irradiance change

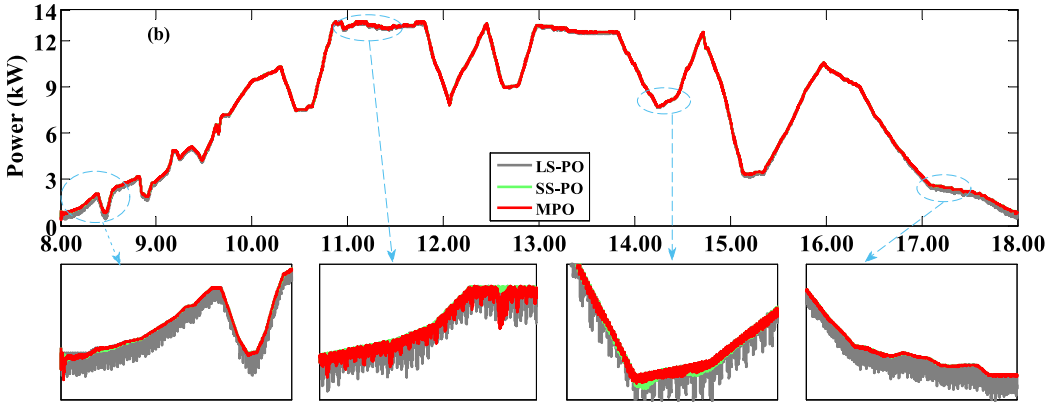

b) PV output voltage

FIGURE 8. Results of realistic irradiance profile

technique exhibits greater oscillation, resulting in increased power losses and reduced tracking efficiency. In contrast, both the small fixed step and proposed MPO techniques demonstrate efficient tracking performance, as evident from

the zoomed-in regions in Fig.8 (b), where changes due to intermittent clouds and showers are captured accurately.

VII. COMPARATIVE STUDY

Table 6 presents a detailed comparison among various MPPT algorithms in terms of perturbation type, controlled variable, converter type, convergence speed, and tracking efficiency to demonstrate the superior tracking performance of the proposed MPO algorithm compared to existing published algorithms. Some P&O algorithms rely on voltage perturbation, which can lead to voltage oscillations, resulting in incorrect tracking, increased computational time, and memory usage. In contrast, the proposed algorithm, like certain other algorithms, utilizes duty cycle perturbation. This approach effectively reduces tracking oscillations and ensures accurate perturbation operation without being affected by voltage oscillations.

The simulation results of [26] closely resemble those of this article, with slight differences in perturbation type, convergence speed, and tracking efficiency. In [26], a voltage perturbation type with variable step-sizes and constant magnitude in each search area is employed. However, this approach can directly influence the tracking process and oscillation levels, particularly during rapid solar radiation fluctuations. Additionally, the algorithm focuses the MPP search area on only 15% of the total curve. Consequently, the proposed MPO algorithm exhibits several advantages over other algorithms, which can be summarized as follows:

- Estimating the open circuit voltage poses a significant challenge.
- The proposed MPO algorithm utilizes the estimated open circuit voltage to guide the tracking process by dividing the power-voltage curve into four regions in both forward and backward perturbation directions. This approach concentrates the search area of the maximum power point (MPP) to only 10% of the total curve.
- When operating below 90% of the power-voltage curve, a large fixed step size is employed to achieve high tracking speed and minimize overall step-size calculations.
- For operation above 90% of the power-voltage curve, the adaptive step-size is applied to ensure minimal oscillations around the MPP.
- The proposed MPO algorithm is designed to operate effectively under various atmospheric conditions.
- The algorithm demonstrates the smallest convergence speed of 15 ms and slightly higher tracking efficiency of the PV system under uniform irradiation (99.8%) with peak-to-peak voltage fluctuations of (V).

VIII. CONCLUSION

This paper has introduced the MPO algorithm, an advanced P&O algorithm designed to improve tracking strategy and performance for achieving high tracking speed and minimal oscillations around MPP. The MPO algorithm enhances the tracking process by dividing the power-voltage curve into four operating areas based on estimated open-circuit voltage. It also reduces unnecessary step-size calculations by limiting the search area to only 10% of the power-voltage curve that contains the MPP. In areas far from the MPP (below 90% of the power-voltage range), a large fixed step-size is used to ensure fast tracking speed.

Furthermore, in the proximity of the MPP, the remaining areas utilize a similar tracking strategy as the adaptive P&O algorithm to achieve minimal voltage fluctuations around the optimal MPP. To assess the effectiveness of the implemented MPO algorithm, MATLAB/SIMULINK simulations are conducted using sinusoidal, ramp irradiance, and one-day (10 hr.) irradiance profiles. The simulation results confirm the superiority of the proposed MPO algorithm over recently published methods, demonstrating the fastest convergence speed (15 ms) and slightly improved tracking efficiency of the PV system under uniform irradiation (99.8%).

For future work, further enhancements can be explored to enhance the performance of the MPO algorithm. One potential direction is to investigate the algorithm's behavior under non-uniform irradiation conditions, such as partial shading or dynamic weather conditions. Additionally, the algorithm could be tested with different types of PV systems and configurations to evaluate its versatility and adaptability. Furthermore, considering the real-world implementation of the algorithm and its integration with hardware controllers should be a focus for future research. Overall, these avenues for future investigation will contribute to a deeper understanding and optimization of the MPO algorithm for improved photovoltaic system performance.

APPENDIX

TABLE 7. Grid-tied PV array parameters.

BC inductance	$L_{BC} = 10\ mH$
BC resistance	$R_{BC} = 0.05\ \Omega$
BC capacitance	$C_{BC} = 14\ \mu F$
BC switching frequency	$F_{SW} = 5\ kHz$
DC inverter reference voltage	$V_{dc\,ref} = 750\ V$
Filter inductance	$L_{Filter} = 2mH$
Filter resistance	$R_{Filter} = 0.015\ \Omega$
Grid voltage	$V_{L.L} = 380\ V$
Grid frequency	$F = 50\ Hz$
BC chopper switch	$IGBT$

TABLE 8. PV array characteristics.

Maximum power, P_{mpp}	13183.22523 W
Voltage at MPP, V_{mpp}	241.5795 V
Current at MPP, I_{mpp}	54.57096 A
Open circuit voltage, V_{oc}	296.309 V
Short circuit current, I_{sc}	61.11132 A
Temperature, at STC	25^oC

REFERENCES

[1] A. I. M. Ali, M. A. Sayed, and E. E. M. Mohamed, "Modified efficient perturb and observe maximum power point tracking technique for grid-tied PV system," *Int. J. Electr. Power Energy Syst.*, vol. 99, pp. 192–202, Jul. 2018.

[2] J. Ahmed and Z. Salam, "An improved perturb and observe (P&O) maximum power point tracking (MPPT) algorithm for higher efficiency," *Appl. Energy*, vol. 150, pp. 97–108, Jul. 2015.

[3] H. H. H. Mousa, A.-R. Youssef, I. Hamdan, M. Ahamed, and E. E. M. Mohamed, "Performance assessment of robust P&O algorithm using optimal hypothetical position of generator speed," *IEEE Access*, vol. 9, pp. 30469–30485, 2021.

[4] N. Femia, G. Petrone, G. Spagnuolo, and M. Vitelli, "A technique for improving P&O MPPT performances of double-stage grid-connected photovoltaic systems," *IEEE Trans. Ind. Electron.*, vol. 56, no. 11, pp. 4473–4482, Nov. 2009.

[5] A. I. M. Ali, M. Abdallah, T. Takeshita, and Z. M. Alaas, "Three-phase single-carrier PWM inverter for isolated grid-tied PV applications," *IEEE Access*, vol. 10, pp. 93395–93411, 2022.

[6] L. Piegari and R. Rizzo, "Adaptive perturb and observe algorithm for photovoltaic maximum power point tracking," *IET Renew. Power Gener.*, vol. 4, no. 4, pp. 317–328, Jul. 2010.

[7] F. Zhang, K. Thanapalan, A. Procter, S. Carr, and J. Maddy, "Adaptive hybrid maximum power point tracking method for a photovoltaic system," *IEEE Trans. Energy Convers.*, vol. 28, no. 2, pp. 353–360, Jun. 2013.

[8] Y. Yang and F. P. Zhao, "Adaptive perturb and observe MPPT technique for grid-connected photovoltaic inverters," *Proc. Eng.*, vol. 23, pp. 468–473, 2011.

[9] M. Kamran, M. Mudassar, M. R. Fazal, M. U. Asghar, M. Bilal, and R. Asghar, "Implementation of improved perturb & observe MPPT technique with confined search space for standalone photovoltaic system," *J. King Saud Univ. Eng. Sci.*, vol. 32, no. 7, pp. 432–441, Nov. 2020.

[10] A. I. M. Ali, M. A. Sayed, and A. A. S. Mohamed, "Seven-level inverter with reduced switches for PV system supporting home-grid and EV charger," *Energies*, vol. 14, no. 9, p. 2718, May 2021.

[11] H.-J. Noh, D.-Y. Lee, and D.-S. Hyun, "An improved MPPT converter with current compensation method for small scaled PV-applications," in *Proc. IEEE 28th Annu. Conf. Ind. Electron. Society*, 2002, pp. 1113–1118.

[12] M. A. S. Masoum, H. Dehbonei, and E. F. Fuchs, "Theoretical and experimental analyses of photovoltaic systems with voltageand current-based maximum power-point tracking," *IEEE Trans. Energy Convers.*, vol. 17, no. 4, pp. 514–522, Dec. 2002.

[13] G. W. Hart, H. M. Branz, and C. H. Cox, "Experimental tests of open-loop maximum-power-point tracking techniques for photovoltaic arrays," *Sol. Cells*, vol. 13, no. 2, pp. 185–195, Dec. 1984.

[14] J. J. Schoeman and J. D. V. Wyk, "A simplified maximal power controller for terrestrial photovoltaic panel arrays," in *Proc. IEEE Power Electron. Specialists Conf.*, Jun. 1982, pp. 361–367.

[15] H. H. H. Mousa, A.-R. Youssef, and E. E. M. Mohamed, "State of the art perturb and observe MPPT algorithms based wind energy conversion systems: A technology review," *Int. J. Electr. Power Energy Syst.*, vol. 126, Mar. 2021, Art. no. 106598.

[16] B. Bendib, H. Belmili, and F. Krim, "A survey of the most used MPPT methods: Conventional and advanced algorithms applied for photovoltaic systems," *Renew. Sustain. Energy Rev.*, vol. 45, pp. 637–648, May 2015.

[17] A. Belkaid, I. Colak, and O. Isik, "Photovoltaic maximum power point tracking under fast varying of solar radiation," *Appl. Energy*, vol. 179, pp. 523–530, Oct. 2016.

[18] A. A. Ghassami, S. M. Sadeghzadeh, and A. Soleimani, "A high performance maximum power point tracker for PV systems," *Int. J. Electr. Power Energy Syst.*, vol. 53, pp. 237–243, Dec. 2013.

[19] M. A. Elgendy, B. Zahawi, and D. J. Atkinson, "Assessment of the incremental conductance maximum power point tracking algorithm," *IEEE Trans. Sustain. Energy*, vol. 4, no. 1, pp. 108–117, Jan. 2013.

[20] H. Fathabadi, "Novel fast dynamic MPPT (maximum power point tracking) technique with the capability of very high accurate power tracking," *Energy*, vol. 94, pp. 466–475, Jan. 2016.

[21] Á.-A. Bayod-Rújula and J.-A. Cebollero-Abián, "A novel MPPT method for PV systems with irradiance measurement," *Sol. Energy*, vol. 109, pp. 95–104, Nov. 2014.

[22] M. Muthuramalingam and P. S. Manoharan, "Comparative analysis of distributed MPPT controllers for partially shaded stand alone photovoltaic systems," *Energy Convers. Manage.*, vol. 86, pp. 286–299, Oct. 2014.

[23] R. Kotti and W. Shireen, "Efficient MPPT control for PV systems adaptive to fast changing irradiation and partial shading conditions," *Sol. Energy*, vol. 114, pp. 397–407, Apr. 2015.

[24] J.-A. Jiang, Y.-L. Su, J.-C. Shieh, K.-C. Kuo, T.-S. Lin, T.-T. Lin, W. Fang, J.-J. Chou, and J.-C. Wang, "On application of a new hybrid maximum power point tracking (MPPT) based photovoltaic system to the closed plant factory," *Appl. Energy*, vol. 124, pp. 309–324, Jul. 2014.

[25] D. Ouoba, A. Fakkar, Y. El Kouari, F. Dkhichi, and B. Oukarfi, "An improved maximum power point tracking method for a photovoltaic system," *Opt. Mater.*, vol. 56, pp. 100–106, Jun. 2016.

[26] A. I. M. Ali and H. R. A. Mohamed, "Improved P&O MPPT algorithm with efficient open-circuit voltage estimation for two-stage grid-integrated PV system under realistic solar radiation," *Int. J. Electr. Power Energy Syst.*, vol. 137, May 2022, Art. no. 107805.

[27] Z. M. Ali, T. Alquthami, S. Alkhalaf, H. Norouzi, S. Dadfar, and K. Suzuki, "Novel hybrid improved bat algorithm and fuzzy system based MPPT for photovoltaic under variable atmospheric conditions," *Sustain. Energy Technol. Assessments*, vol. 52, Aug. 2022, Art. no. 102156.

[28] C. Gonzalez-Castano, C. Restrepo, S. Kouro, and J. Rodriguez, "MPPT algorithm based on artificial bee colony for PV system," *IEEE Access*, vol. 9, pp. 43121–43133, 2021.

[29] H. Tao, M. Ghahremani, F. W. Ahmed, W. Jing, M. S. Nazir, and K. Ohshima, "A novel MPPT controller in PV systems with hybrid whale optimization-PS algorithm based ANFIS under different conditions," *Control Eng. Pract.*, vol. 112, Jul. 2021, Art. no. 104809.

[30] J. Aguila-Leon, C. Vargas-Salgado, C. Chiñas-Palacios, and D. Díaz-Bello, "Solar photovoltaic maximum power point tracking controller optimization using grey wolf optimizer: A performance comparison between bio-inspired and traditional algorithms," *Exp. Syst. Appl.*, vol. 211, Jan. 2023, Art. no. 118700.

[31] S. Manna, A. K. Akella, and D. K. Singh, "Implementation of a novel robust model reference adaptive controller-based MPPT for stand-alone and grid-connected photovoltaic system," *Energy Sources, A, Recovery, Utilization, Environ. Effects*, vol. 45, no. 1, pp. 1321–1345, Apr. 2023.

[32] I. Houssamo, F. Locment, and M. Sechilariu, "Maximum power tracking for photovoltaic power system: Development and experimental comparison of two algorithms," *Renew. Energy*, vol. 35, no. 10, pp. 2381–2387, Oct. 2010.

[33] J. Ahmad, "A fractional open circuit voltage based maximum power point tracker for photovoltaic arrays," in *Proc. 2nd Int. Conf. Softw. Technol. Eng.*, vol. 1, Oct. 2010, pp. V1-247–V1-250.

[34] T. Esram and P. L. Chapman, "Comparison of photovoltaic array maximum power point tracking techniques," *IEEE Trans. Energy Convers.*, vol. 22, no. 2, pp. 439–449, Jun. 2007.

[35] K. Kobayashi, H. Matsuo, and Y. Sekine, "A novel optimum operating point tracker of the solar cell power supply system," in *Proc. IEEE 35th Annu. Power Electron. Specialists Conf.*, 2004, pp. 2147–2151.

[36] J. H. R. Enslin, M. S. Wolf, D. B. Snyman, and W. Swiegers, "Integrated photovoltaic maximum power point tracking converter," *IEEE Trans. Ind. Electron.*, vol. 44, no. 6, pp. 769–773, 1997.

[37] A. K. Abdelsalam, A. M. Massoud, S. Ahmed, and P. N. Enjeti, "High-performance adaptive perturb and observe MPPT technique for photovoltaic-based microgrids," *IEEE Trans. Power Electron.*, vol. 26, no. 4, pp. 1010–1021, Apr. 2011.

[38] M. M. Algazar, H. Al-Monier, H. A. El-halim, and M. E. El Kotb Salem, "Maximum power point tracking using fuzzy logic control," *Int. J. Elect. Power Energy Syst.*, vol. 39, no. 1, pp. 21–28, 2012.

[39] A. Amir, A. Amir, J. Selvaraj, N. A. Rahim, and A. M. Abusorrah, "Conventional and modified MPPT techniques with direct control and dual scaled adaptive step-size," *Sol. Energy*, vol. 157, pp. 1017–1031, Nov. 2017.

[40] Q. Mei, M. Shan, L. Liu, and J. M. Guerrero, "A novel improved variable step-size incremental-resistance MPPT method for PV systems," *IEEE Trans. Ind. Electron.*, vol. 58, no. 6, pp. 2427–2434, Jun. 2011.

AHMED ISMAIL M. ALI (Member, IEEE) was born in Qena, Egypt, in 1991. He received the B.Sc. and M.Sc. degrees in electrical engineering from the Faculty of Engineering and Technology, South Valley University, Qena, in 2013 and 2017, respectively, and the Ph.D. degree in electrical engineering from the Nagoya Institute of Technology, Nagoya, Japan, in 2022.

Since 2013, he has been with the Department of Electrical Engineering, Faculty of Engineering, South Valley University, as an Administrator and a Research Assistant, since 2017, where he is currently an Assistant Professor with the Department of Electrical Engineering, South Valley University. He has coauthored number of publications, including PWM DC/AC inverters, bidirectional inverters, and DC/DC converters, in addition to advanced MPPT techniques for PVs and WECSs. His research interests include power electronic converters, PWM techniques, DC/AC and AC/DC converters, modular multilevel converters (MMxC), control systems, and renewable energy applications, in addition to battery chargers for electric vehicle applications.

Dr. Ali is a Graduate Student Member of the Institute of Electrical Engineers of Japan (IEEJ). He is a member of the IEEE Power Electronics Society (PELS) and IEEE Industry Application Society (IAS). He has been awarded the South Valley University Prize for international publishing, in 2018 and 2023.

HOSSAM H. H. MOUSA was born in Qena, Egypt, in 1994. He received the B.Sc. and M.Sc. degrees in electrical power and machines engineering from South Valley University, Qena, in 2017 and 2020, respectively. In 2018, he joined the Department of Electrical Engineering, Faculty of Engineering, South Valley University, as a Teaching Assistant, where he is currently an Assistant Lecturer. His research interests include electrical power engineering, MPPT techniques for renewable energy systems, microgrid energy management, and control systems.

HASSANIEN RAMADAN A. MOHAMED was born in Qena, Egypt, in 1992. He received the B.Sc. degree from the Faculty of Engineering and Technology, South Valley University, Qena, in 2013, and the M.Sc. degree from the Budapest University of Technology and Economics, Budapest, Hungary, in 2018. He is currently pursuing the Ph.D. degree with the Department of Electrical and Computer Engineering, University of Alberta, Canada. His research interests include dynamics and control of power electronic converters for MTDC grids and optimal grid integration of renewable energy resources and electric vehicles.

SALAH KAMEL received the international Ph.D. degree from Jaen University, Spain (Main), and Aalborg University, Denmark (Host), in January 2014. He is currently an Associate Professor with the Department of Electrical Engineering, Aswan University. He is also the Leader of the Advanced Power Systems Research Laboratory (APSR Lab), Power Systems Research Group, Aswan, Egypt. His research interests include power system analysis and optimization, smart grids, and renewable energy systems.

ABDURRAHMAN SHUAIBU HASSAN received the Ph.D. degree in electrical electronics engineering. He is currently a Senior Lecturer with the Department of Electrical Engineering, School of Engineering and Applied Sciences, Kampala International University. He is passionate about academia, the industry, research, and development and has always strived to join and become part of a competitive program which meets long-term educational and research needs, to drive a scientific approach to engineering processes. His research interests include power system analysis and optimizations, the economics of power systems, smart grids, energy, and nonconventional energy systems.

ZUHAIR MUHAMMED ALAAS (Member, IEEE) received the B.S. degree from the King Fahd University of Petroleum and Minerals (KFUPM), Dhahran, Saudi Arabia, in 2002, the M.S. degree from the University of Newcastle upon Tyne, Newcastle, U.K. in 2007, and the Ph.D. degree from Wayne State University, Detroit, Michigan, USA, in 2017, all in electrical engineering. From September 2002 to November 2010, he was a Lecturer with the Abha College, Technical and Vocational Training Corporation, Saudi Arabia. From November 2010 to June 2011, he was a Power Transmission Engineer with Saudi Electric Company. Since June 2011, he has been with Jazan University, where he is currently an Assistant Professor and the Department of Electrical Engineering Chairperson. His current research interests include energy storage devices, power electronics, microgrids, alternative/hybrid energy power generation systems, and motor drives.

ESSAM E. M. MOHAMED (Member, IEEE) was born in Qena, Egypt, in 1974. He received the B.Sc. and M.Sc. degrees in electrical power and machines engineering from the Faculty of Energy Engineering, Aswan University, Aswan, Egypt, in 1997 and 2003, respectively, and the Ph.D. degree in electrical engineering from The University of Sheffield, Sheffield, U.K., in 2011.

In 1999, he joined the Department of Electrical Engineering, Faculty of Energy Engineering, Aswan University. Since 2013, he has been with the Department of Electrical Engineering, Faculty of Engineering, South Valley University, Qena. He is currently the Founder and the Manager of the South Valley University IEEE Student Branch. His research interests include power electronics, electrical machines design and control, electric drives, and renewable energy systems.

ABDEL-RAHEEM YOUSSEF ABDALLAH was born in Qena, Egypt, in 1984. He received the B.Sc. and M.Sc. degrees in electrical engineering from Aswan University, Aswan, Egypt, in 2005 and 2011, respectively, and the Ph.D. degree in electrical engineering from the Ismailia Faculty of Engineering, Suez Canal University, Egypt, in 2017. Currently, he is an Assistant Professor with the Department of Electrical Engineering, Faculty of Engineering, South Valley University, Qena. His research interests include optimization of power systems and integration renewable energy resources into utility grid. He has been awarded the South Valley University Prize for international publishing, in 2018 and 2021. Also, he received the South Valley University Encouragement Award, in 2020.